RESEARCH ARTICLE

Design, synthesis, in vitro evaluation, and molecular modeling studies of *N*-substituted benzomorphans, analogs of LP2, as novel MOR ligands

Giuliana Costanzo[1] | Vincenzo Patamia[2] | Rita Turnaturi[2] | Carmela Parenti[2] | Chiara Zagni[2] | Jessica Lombino[2] | Emanuele Amata[2] | Agostino Marrazzo[2] | Lorella Pasquinucci[2] | Antonio Rescifina[2] 🄳

[1]Department of Biomedical and Biotechnological Sciences, University of Catania, Catania, Italy

[2]Department of Drug and Health Sciences, University of Catania, Catania, Italy

Correspondence
Lorella Pasquinucci, Department of Drug and Health Sciences, University of Catania, Catania, Italy.
Email: lpasquin@unict.it

Funding information
University of Catania

Abstract

6,7-Benzomorphans have been investigated in medicinal chemistry for developing new drugs. This nucleus could be considered a versatile scaffold. The physicochemical properties of benzomorphan *N*-substituent are crucial in achieving a definite pharmacological profile at opioid receptors. Thus, the dual-target MOR/DOR ligands LP1 and LP2 were obtained through *N*-substituent modifications. Specifically, LP2, bearing as *N*-substituent the (2*R/S*)-2-methoxy-2- phenylethyl group, is a dual-target MOR/DOR agonist and is successful in animal models of inflammatory and neuropathic pain. To obtain new opioid ligands, we focused on the design and synthesis of LP2 analogs. First, the 2-methoxyl group of LP2 was replaced by an ester or acid functional group. Then, spacers of different lengths were introduced at *N*-substituent. In-vitro, their affinity profile versus opioid receptors has been performed through competition binding assays. Molecular modeling studies were conducted to deeply analyze the binding mode and the interactions between the new ligands and all opioid receptors.

KEYWORDS
6,7-benzomorphan, docking studies, opioid receptor, radioligand competition-binding

1 | INTRODUCTION

6,7-Benzomorphans, originated from morphine structure simplification, have been investigated in medicinal chemistry for developing new drugs (Turnaturi et al., 2018). In the interaction of opioid receptors with benzomorphan-based compounds, three different pharmacophoric requirements were identified: the aromatic ring, the saturated segment, and the basic nitrogen. In fact, the basic nitrogen and phenolic group of Tyr1 of endogenous opioid peptides could be mimic by the rigid benzomorphan scaffold. The (−)-(2*R*,6*R*,11*R*) configuration of the benzomorphan nucleus is preferred for opioid receptors interaction and is identical to the (−)-morphine configuration (Pathan & Williams, 2012). Moreover, this nucleus could be considered a versatile scaffold, and the

Giuliana Costanzo and Vincenzo Patamia contributed equally to this work.

modifications of the functional groups attached to basic nitrogen led to different opioid ligands. Thus, the physico-chemical properties of benzomorphan *N*-substituent are crucial in achieving a definite pharmacological profile at MOR (mu opioid receptor), DOR (delta opioid receptor), and KOR (kappa opioid receptor).

To obtain different functional profiles, Pasquinucci et al. (Pasquinucci et al., 2021) designed and synthesized different benzomorphan-based compounds. The dual-target MOR/DOR ligands **LP1** and **LP2** were discovered (Figure 1). **LP1**, bearing an *N*-phenylpropanamide substituent (Pasquinucci et al., 2010), is a potent MOR agonist/DOR antagonist able to counteract nociceptive pain and behavioral signs of persistent pain with low tolerance-inducing capability (Parenti et al., 2013; Pasquinucci et al., 2012). Moreover, **LP2**, with a flexible 2-methoxyethyl spacer at *N*-substituent, is a dual-target MOR/DOR agonist (Pasquinucci et al., 2017) that exhibited antinociceptive effect in nociceptive and persistent pain models (Pasquinucci et al., 2019; Vicario et al., 2019). Thus, **LP1** and **LP2** could represent helpful examples of the discovery process of new opioid ligands with a safer profile through *N*-substituent modification of the benzomorphan scaffold.

To improve the understanding of molecular interaction between the *N*-substituent and the opioid receptors, here we report the design and synthesis of **LP2** analogs. First, the structure-affinity profile of new ligands was evaluated, and the 2-methoxyl group of **LP2** was replaced by an ester or acid functional group. Then, spacers of different lengths were introduced at *N*-substituent (Figure 1). In all new **LP2** analogs the phenyl ring in the *N*-substituent of the benzomorphan scaffold was retained. In-vitro, their affinity profile versus opioid receptors has been performed through competition binding assays. Molecular modeling was conducted to deeply analyze the binding mode and the interactions between the new ligands and MOR, DOR, and KOR.

2 | RESULTS AND DISCUSSION

2.1 | Chemistry

The new compounds **2**, **3**, and **10**–**13** were synthesized according to Schemes 1 and 2, respectively. Compound **1** was prepared by primary alcohol sulfonylation with methane-sulfonyl chloride and triethylamine in CH_2Cl_2. Target ester **2** was obtained by alkylation of (−)-*cis*-*N*-normetazocine (Brine et al., 1990) with the mesylated alcohol **1**, and the respective acid derivate **3** was obtained by the ester hydrolysis in basic condition.

Intermediate compounds **8** and **9** were synthesized as previously reported (Cheng et al., 1990). Target compounds **10** and **11** were synthesized by alkylation of (−)-*cis*-*N*-normetazocine with intermediate compounds **8** and **9**. The respective acids **12** and **13** were obtained by esters hydrolysis in basic condition. New synthesized compounds possess a chiral stereocenter at the *N*-substituent of (−)-*cis*-*N*-normetazocine scaffold and are a mixture of diastereoisomers, not separable in our purification procedures. They were characterized by ^1H NMR, ^{13}C NMR, and elemental analysis.

2.2 | Radioligand binding assays

Target compounds **2**, **3**, and **10**–**13** were assayed on opioid receptors, as previously described (Rita Turnaturi et al., 2022). Inhibition constant (K_i) values (Table 1) were calculated using nonlinear regression analysis (GraphPad Prism, version 6.0, GraphPad Software In.). (Figures S1–S3).
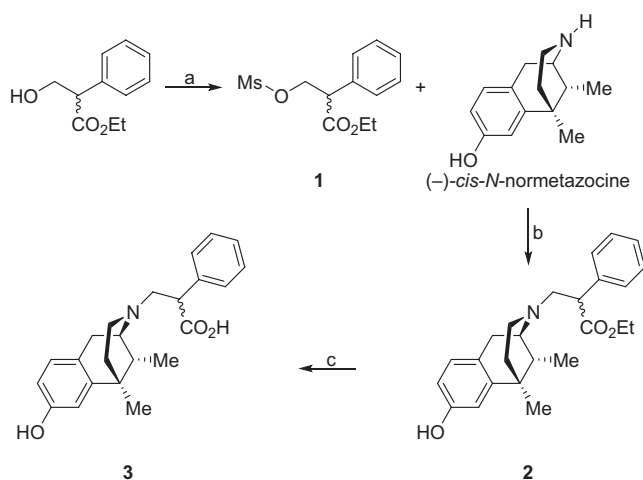
Compared to **LP2**, K_i values versus MOR, DOR, and KOR are higher for all newly synthesized compounds. However, regarding their affinity to opioid receptors, the new molecules behaved differently based on *N*-substituents. **LP2** has the phenyl ring in the *N*-substituent of the benzomorphan scaffold linked to an ethyl spacer bearing a methoxyl group at carbon 2. In compound **2**, the 2-methoxyl group of **LP2** was replaced by an ethyl ester functional group. This substitution is well tolerated, and compound **2** confirmed a MOR profile with the K_i values of 38.2 nM. Instead, a reduction of DOR and KOR affinity in comparison to **LP2** was observed. Compounds **10** and **11** also retained an ethyl ester functionality in *N*-substituent, but the distance with respect to basic nitrogen of the benzomorphan nucleus was incremented by 1 and 2 methylene units, respectively. The nanomolar MOR affinity, exhibited by compounds **10** and **11** ($K_i = 10$ nM

FIGURE 1 Chemical structures of **LP1**, **LP2** and the newly synthesized compounds.
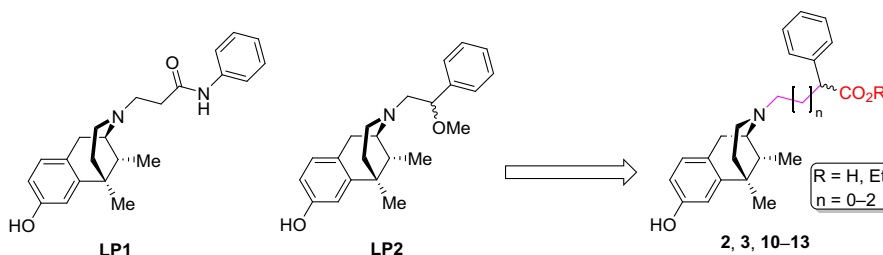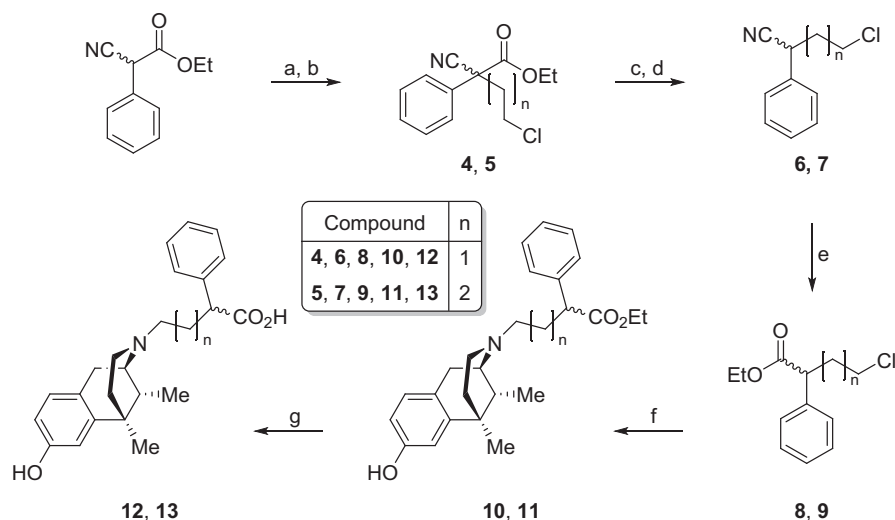
and $K_i = 53.7$ nM, respectively), confirmed that in MOR interaction, the ethyl ester in *N*-substituent was tolerated highlighting an optimal two methylene units spacer. In compounds **10** and **11**, the affinity at DOR (14- and 50-fold, respectively) and KOR (2- and 6-fold) was higher with respect to compound **2**, with a significative incremental of KOR affinity in compound **11** ($K_i = 32.1 \pm 4$), showing a selectivity ratio of $K_i^{DOR}/K_i^{MOR} = 2.31$ and $K_i^{KOR}/K_i^{MOR} = 0.6$.

An acid functional group characterizes the compounds **3**, **12**, and **13**. Compound **12** showed a nanomolar K_i value at MOR comparable to its ester analog **10**. Instead, the acid functional group in compounds **3** and **13** led to a detrimental effect on all opioid receptors compared to compounds **2** and **11**. Thus, replacing the ester group with the corresponding acid group seems not tolerated depending on chain lengths.

SCHEME 1 Synthesis of target compounds **2** and **3**. Reagents and conditions: (a) MsCl, TEA, anhydrous DCM, rt, 3 h; (b) NaHCO₃, KI, DMF, 55 °C, 24 h; (c) NaOH 1 N, 110 °C, 5 h.

2.3 | Molecular modeling

2.3.1 | Docking studies

In silico studies were performed using AutoDock implemented in the YASARA software. The docking studies were performed on all the protonation states of the compounds at pH 7.4, previously calculated using the Marvin software (Rescifina et al., 2014; Szczepańska et al., 2021; Varrica et al., 2018).
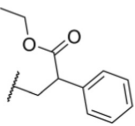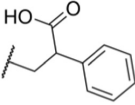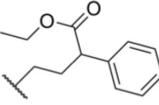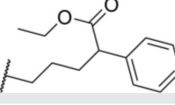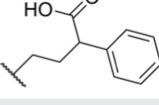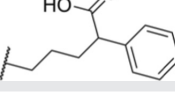
All compounds at pH 7.4 possess positively charged nitrogen, forming a nitrogen stereocenter for each molecule in addition to the one already present. To avoid docking studies on four stereoisomers for each compound, we first docked the four stereoisomers of compound **LP2**, using it as a reference (Figure 2). Then, regarding the nitrogen stereocenter, the chosen stereoisomer had the calculated K_i value closest to the experimental one, in our case (*R*)-*N*. Based on this assumption, we kept the stereocenter on nitrogen fixed (*R*) for all other compounds and performed docking studies on the two isomers of each compound for the three receptors.

In Table 2, we have only listed the ΔG and K_i values of the isomers whose calculated K_i value is closest to the experimental one; in almost all compounds, however, there is not much difference in inhibitory activity between the two isomers.

Focusing on the MOR, we carefully analyzed the poses within the receptor site of compounds **10** and **12**, which possess a ΔG (kcal/moL) of −9.91 and −9.67, respectively.

In Figure 3, we show the 3D and 2D poses of compounds **10**, **12**, and LP2 within the MOR, where we can see that the presence of the two groups, ester, and carboxylic acid, alters the pose within the site but still retains excellent inhibitory activity. Compound **10** (Figure 3a), in addition to hydrophobic interactions with residues Ile296 and 322, in common with compound **12**, possesses a salt

Compound	n
4, 6, 8, 10, 12	1
5, 7, 9, 11, 13	2

SCHEME 2 Synthesis of target compounds **10–13**. Reagents and conditions: (a) *t*-BuOK, anhydrous DMF, rt, 0.5 h; (b) 1-bromo-2-chloroethane (*n* = 1) or 1-chloro-3-iodopropane (*n* = 2), rt, 24 h; (c) K₂CO₃, MeOH, rt, 3 h; (d) HCl 1 N; (e) HCl/EtOH 1:1, rt, 24 h; (f) (−)-*cis*-*N*-normetazocine, NaHCO₃, KI, DMF, 55 °C, 24 h; (h) NaOH 1 N, 110 °C, 5 h.

TABLE 1 Opioid receptors binding affinity and selectivity of compounds **2**, **3**, and **10–13**.

Compound	N-substituent	K_i (nM) ± SD[a]			K_i^{DOR}/K_i^{MOR}	K_i^{KOR}/K_i^{MOR}
		MOR	DOR	KOR		
2		38.2 ± 4	6,170 ± 70	211.0 ± 10	161.5	5.5
3		980.6 ± 8	2,769.0 ± 50	715.0 ± 4	2.8	0.7
10		10.8 ± 2	440.0 ± 22	130.0 ± 15	40.7	12.0
11		53.7 ± 7	124.0 ± 8	32.1 ± 4	2.3	0.6
12		11.8 ± 2	275.0 ± 11	3,216.0 ± 60	23.3	252.7
13		477.0 ± 27	852.0 ± 10	2,716.0 ± 20	1.8	4.6
2R/S-**LP2**[b]		1.1 ± 0.1	6.6 ± 0.6	15.2 ± 0.8	6.1	14.0
DAMGO		1.2 ± 0.1	—	—	—	—
Naltrindole		—	1.1 ± 0.1	—	—	—
U69,593		—	—	0.3 ± 0.1	—	—

[a]Each value is the mean ± SD of at least two experiments performed in duplicate. Reference compounds were tested with the same membrane homogenates.
[b]Reference (Pasquinucci et al., 2017).

bridge with residue Asp147, a typical interaction for the MOR; it also establishes hydrogen bonds with residues Gln124 and Asn127. The presence of the carboxyl group in compound **12**, on the other hand, allows the formation of a hydrogen bond with His297 and prevents the formation of the salt bridge with Asp147, with which electrostatic interactions are formed (Ricarte et al., 2021; Zádor et al., 2022) (Figure 3b).

Another aspect being emphasized is the different affinity that **10** and **12** have compared to the other ligands studied; this is to be found in the spacer chain. The presence of an alkyl chain of two carbon atoms allows ligands **10** and **12** to accommodate themselves within the receptor site in such a way as to maximize interactions and strengthen anchoring.

2.3.2 | Molecular dynamics

To study better the formation of the ligand@protein complex, 100 ns molecular dynamics of ligands **10** and **12** were performed within the receptor pocket of the MOR protein. From the graphs of the total energy and RMSD (root-mean-square deviation) of the complexes (Figure 4), it is clear that both ligands form a very stable complex with the MOR; this is due to the dense network of interactions, previously commented, that keep the ligands anchored within the receptor pocket (Gentile et al., 2022).

3 | CONCLUSION

Novel **LP2** analogs with a benzomorphan scaffold were designed and synthesized. Based on in vitro competition binding assays and molecular modeling studies, compounds **10** and **12** showed a high affinity for MOR. Both molecules are appropriately located in the binding pocket of MOR, and maintain a similar docking pose. An alkyl chain of two methylene units maximizes their interactions with MOR, highlighting the critical role of the distance between the basic nitrogen of the benzomorphan scaffold

and the ester or acid functional groups. Thus, the combination of different functional groups and the spacing carbon chain length appeared to determine the affinity profile of compounds. In this study, we confirmed that *N*-substituent nature modulates the nature of interactions towards the opioid receptors.
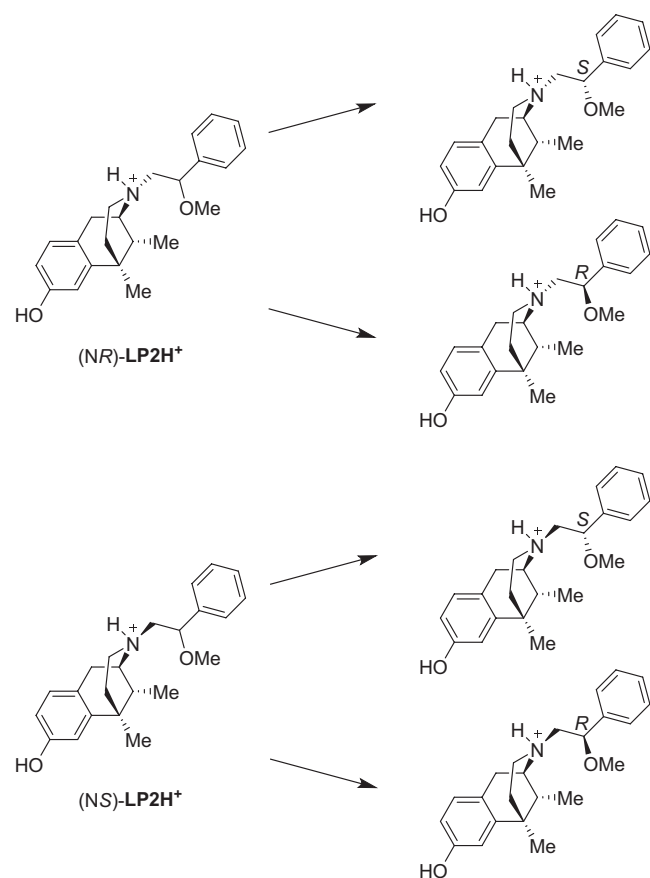

FIGURE 2 Protonation states of **LP2** and relative stereoisomers.

4 | EXPERIMENTAL SECTION

4.1 | General remarks

Reagent-grade chemicals were purchased from Merck (Darmstadt, Germany) and (±)-*cis*-*N*-normetazocine was obtained from Fabbrica Italiana Sintetici. All new compounds were purified by flash column chromatography on Merck silica gel 60 (230–400 mesh). Melting points were determined in open capillary tubes with a Büchi 530 apparatus and are uncorrected. Optical rotations were determined in EtOH solution with a Perkin-Elmer 241 polarimeter. ^{1}H and ^{13}C NMR spectra were recorded at 200 and 500 MHz on Varian Inova spectrometers in $CDCl_3$, CD_3OD or DMSO-d_6. Elemental analyses (C, H, N) were performed on a Carlo Erba 1106 analyzer, and the results were within ±0.4% of the theoretical values.

4.2 | Preparation of the target compounds 2 and 3

4.2.1 | Ethyl 3-((methylsulfonyl)oxy)-2-(*R/S*)-phenylpropanoate (**1**)

Ethyl tropate (2.77 mmoL, 1 eq) was dissolved in CH_2Cl_2 (6 mL), the solution was cooled at 0 °C under a nitrogen atmosphere, and triethylamine (5.54 mmoL, 2 eq) and methanesulfonyl chloride (3.33 mmoL, 1.2 eq) were added. The reaction mixture was stirred overnight at rt. After, the mixture was transferred to a separatory funnel and partitioned (CH_2Cl_2/H_2O). The organic phase was washed with brine, dried over Na_2SO_4, and concentrated in vacuo to give an amber oil that, purified by flash chromatography (EtOAc/C_6H_{12} 1:9), gave a light-yellow oil. Yield: 42%; TLC EtOAc/C_6H_{12} (2:8 *v/v*) $R_f = 0.50$; ^{1}H NMR

TABLE 2 Calculated free energies of binding, ΔG (kcal/moL), and constants of binding, K_i (nM), for the binding sites of MOR, DOR, and KOR for all compounds.

Compound	MOR			DOR			KOR		
	Calcd ΔG	Calcd K_i	Expected K_i	Calcd ΔG	Calcd K_i	Expected K_i	Calcd ΔG	Calcd K_i	Expected K_i
2	−9.86	58.7	38.2 ± 4	−6.97	7733.4	6170.0 ± 70	−9.16	191.5	211.0 ± 10
3	−8.04	1269.6	980.6 ± 8	−7.58	2760.7	2769.0 ± 50	−8.34	765.0	715 ± 4
10	−9.91	54.0	10.8 ± 2	−8.59	501.5	440 ± 22	−9.32	146.2	130 ± 15
11	−9.78	67.2	53.7 ± 7	−8.78	363.9	124 ± 8	−9.89	55.8	32.1 ± 4
12	−9.67	81.0	11.8 ± 2	−8.96	268.5	275 ± 11	−7.57	2807.7	3216 ± 60
13	−8.69	423.6	477 ± 27	−8.20	969.0	852 ± 10	−7.74	2107.0	2716 ± 20
2R/S-LP2	−9.64	85.2	1.08 ± 0.10	−9.86	58.7	6.61 ± 0.60	−9.13	212.0	15.22 ± 0.80
DAMGO	−11.83	2.1	1.16 ± 0.10		–			–	
Naltrindole		–		−9.68	79.6	1.13 ± 0.10		–	
U69,593		–			–		−9.91	54.0	0.34 ± 0.10

FIGURE 3 3D and 2D poses of compounds **10** (a), **12** (b), and LP2 (c) within the MOR binding site.
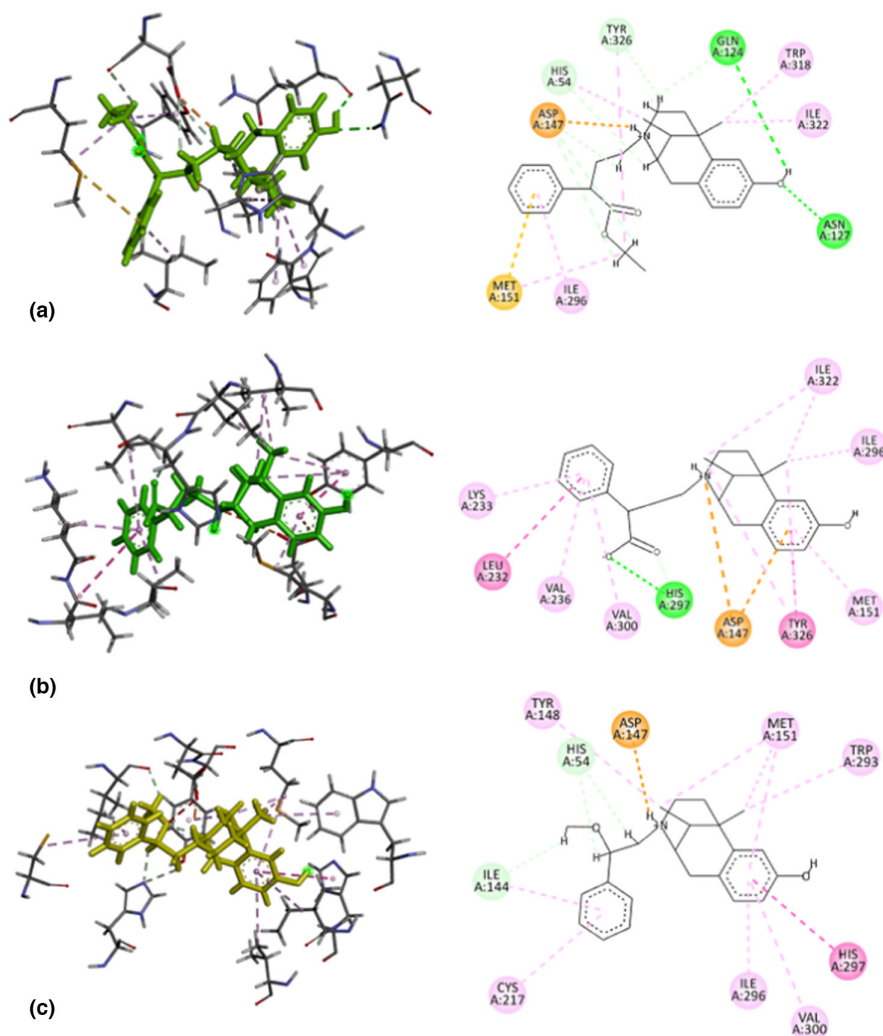
(200 MHz, CDCl$_3$): δ = 7.34–7.21 (m, 5H), 4.56–4.47 (m, 1H), 4.21–4.06 (m, 1H), 3.73–3.68 (m, 3H), 2.97 (s, 3H), 1.21 (t, 3H).

4.2.2 | Ethyl 3-((2R,6R,11R)-8-hydroxy-6,11-dimethyl-1,4,5,6-tetrahydro-2,6-methanobenzo[d]azocin-3(2H)-yl)-2-(R/S)-phenylpropanoate (2)

(−)-*cis*-N-normetazocine (0.92 mmol, 1 eq) was dissolved in DMF (5 mL) and ethyl 3-((methylsulfonyl)oxy)-2-phenylpropanoate (0.92 mmol, 1 eq), NaHCO$_3$ (1.38 mmoL, 1.5 eq) and KI (catalytic quantity) were added. The reaction mixture was stirred overnight at 55 °C. At the reaction mixture, 4 mL of H$_2$O were added, and the aqueous phase was extracted with EtOAc; the organic phase was dried over Na$_2$SO$_4$ and concentrated in vacuo. The reaction crude was purified by flash chromatography (CH$_2$Cl$_2$/MeOH 95:5) to obtain a white solid. Yield: 96%; Mp: 178–181 °C; $[\alpha]_D^{25}$ = −61.7° (c 1.005, EtOH); TLC CH$_2$Cl$_2$/MeOH (95:5 v/v) R_f = 0.49; ^{1}H NMR

(500 MHz, CDCl$_3$): δ = 7.40–7.25 (m, 5H), 6.87 (d, 1H, J = 8.3 Hz), 6.70 (d, 1H, J = 3.4 Hz), 6.60 (dd, 1H, J = 8.3, 3.4 Hz), 5.90 (s, 1H), 4.25 (d, 2H, J = 7.2 Hz), 3.28 (d, 1H, J = 7.1 Hz), 2.99–2.79 (m, 4H), 2.70–2.59 (m, 4H), 1.84–1.70 (m, 2H), 1.29 (s, 3H), 1.27 (t, 3H, J = 7.2 Hz), 0.80 (d, 3H, J = 7.0). (Figure S4) ^{13}C NMR (125 MHz, CDCl$_3$): δ = 173.95, 154.46, 137.41, 18.98, 128.51, 128.26, 128.12, 128.09, 128.00, 127.94, 127.33, 126.88, 113.89, 112.83, 112.43, 112.23, 66.12, 57.18, 51.80, 51.31, 46.24, 45.75, 42.20, 41.96, 41.46, 36.40, 25.55, 24.79, 14.17, 13.55. Anal (C$_{25}$H$_{31}$NO$_3$) C, H, N (Table S1).

4.2.3 | 3–[(2R,6R,11R)–8-hydroxy-6,11-dimethyl-1,4,5,6-tetrahydro-2,6-methanobenzo[d]azocin-3(2H)-yl]-2(R/S)-phenylpropanoic acid (3).

1 N NaOH solution (3.06 mmol, 9.27 eq) was added to ethyl 3-((2R,6R,11R)-8-hydroxy-6,11-dimethyl-1,4,5,6-tetrahydro-2,6-methanobenzo[d]azocin-3(2H)yl)-2-phenylpropanoate (0.33 mmoL, 1 eq). The resulting suspension was vigorously
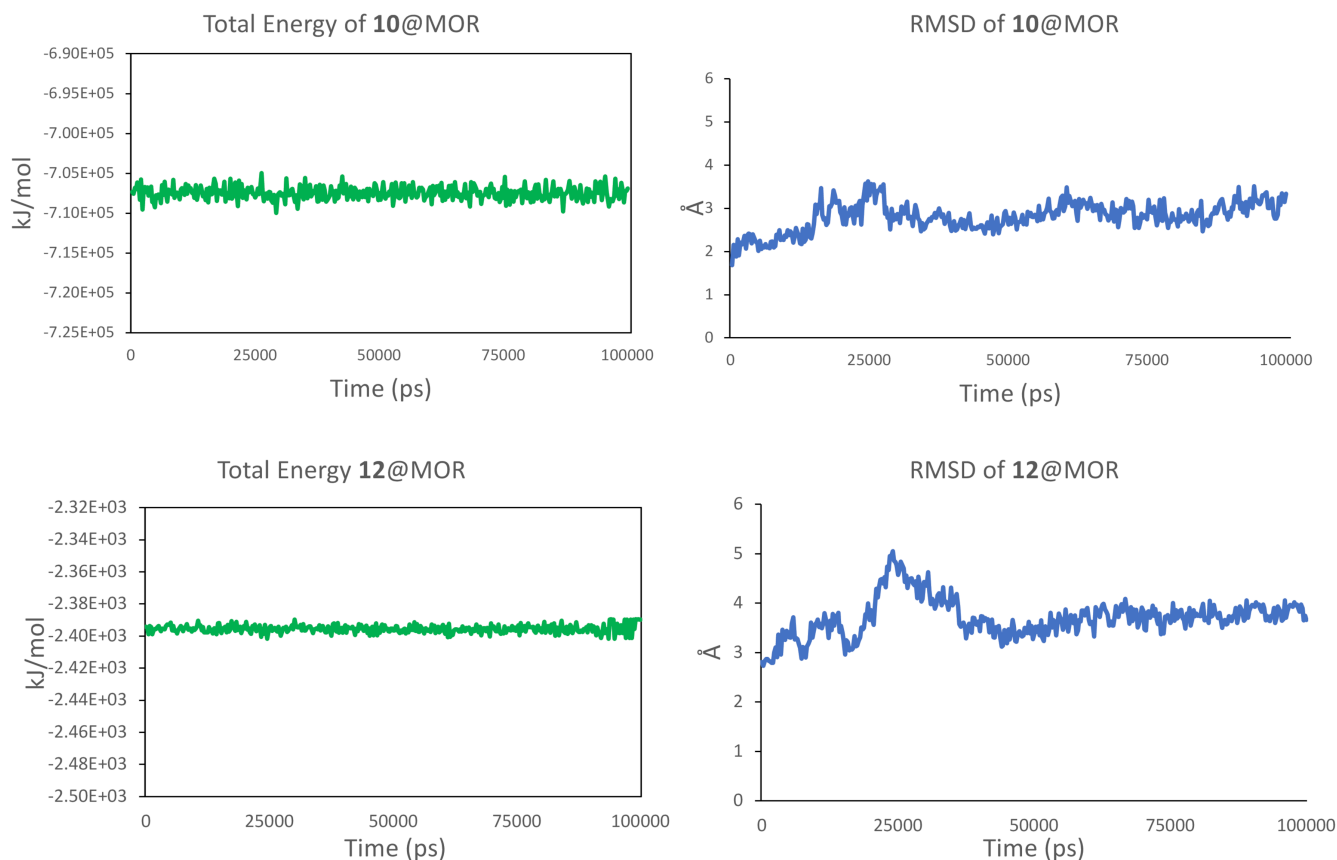
FIGURE 4 Total energy and RMSD of the ligand@protein complexes for compounds **10** (upper) and **12** (down) within the MOR.

stirred and refluxed at 110 °C for 5 h. After cooling, the re-action mixture was partitioned (CHCl$_3$/H$_2$O). A 1 N solution of HCl was added to the aqueous phase to a pH of 5–6. The obtained yellow precipitate was crystallized by EtOH/ diethyl ether. Yield: 90%; Mp: 180–183 °C; $[\alpha]_D^{25} = -57.2°$ (c 1.03, EtOH); TLC CH$_2$Cl$_2$/MeOH (95:5 v/v): $R_f = 0.30$; ^{1}H NMR (500 MHz, DMSO-d_6): $\delta = 9.12$ (br, 1H), 7.31–7.28 (m, 5H), 6.87–6.84 (m, 1H), 6.60–6.59 (m, 1H), 6.55–6.53 (m, 1H), 4.11–3.98 (m, 1H), 3.30–3.19 (m, 4H), 3.01–2.74 (m, 3H), 2.35–2.24 (m, 1H), 1.99–1.76 (m, 2H), 1.23 (s, 3H), 0.72 (d, 3H). (Figure S5) ^{13}C NMR (125 MHz, DMSO-d_6): $\delta = 173.44, 155.95, 140.66, 137.81, 128.54, 128.48, 128.06, 128.02, 127.94, 127.88, 127.22, 126.04, 113.50, 111.83, 92.52, 56.26, 51.00, 46.74, 45.08, 35.17, 26.58, 25.39, 12.93$. Anal (C$_{23}H_{27}NO_3$) C, H, N (Table S1).

4.3 | Preparation of the target compounds 10–13

4.3.1 | Ethyl 4-chloro-2-(R/S)-cyano-2-phenylbutanoate (4)

To a suspension of potassium t-butoxide (34 mmoL, 2 eq) in anhydrous DMF (18 mL), ethyl phenyl cyanoacetate

(17 mmoL, 1 eq) was added dropwise, under argon. After 30 min, 1-bromo-2-chloroethane (25.5 mmoL, 1.5 eq) was added dropwise. The reaction mixture was stirred at rt for 24 h. Then, the DMF is removed under vacuum. To the reaction mixture, an aqueous solution of NH$_4$Cl was added. The mixture was transferred to a separatory fun-nel and partitioned with diethyl ether. The crude obtained was purified by flash chromatography on silica gel (C$_6$H$_{12}$/ EtOAc, 9:1–8:2) to give a yellow oil. Yield: 63.25%. TLC C$_6$H$_{12}$/EtOAc (8:2 v/v): $R_f = 0.33$; ^{1}H NMR (200 MHz, CDCl$_3$): $\delta = 7.56$–7.40 (m, 5H), 4.28 (q, 1H, $J = 7.2$ Hz), 4.21 (q, 1H, $J = 7.2$ Hz), 3.71–3.45 (m, 2H), 2.96–2.81 (m, 1H), 2.68–2.53 (m, 1H), 1.25 (t, 3H, $J = 7.2$ Hz).

4.3.2 | Ethyl 5-chloro-2-(R/S)-cyano-2-phenylpentanoate (5)

To a suspension of potassium t-butoxide (42.28 mmoL, 2 eq) in anhydrous DMF (18 mL), ethyl phenyl cyanoac-etate (21.14 mmoL, 1 eq) was added dropwise, under argon. After 30 min, 1-chloro-3-iodopropane (41.10 mmoL, 1.5 eq) was added dropwise. The reaction mixture was stirred at rt for 24 h. Then, the DMF is removed under vacuum. To the reaction mixture, an aqueous solution of NH$_4$Cl was added.

The mixture was transferred to a separatory funnel and partitioned with diethyl ether. The crude obtained was purified by flash chromatography on silica gel (C$_6$H$_{12}$/EtOAc, 9:1–8:2) to give a yellow oil. Yield: 54%; TLC C$_6$H$_{12}$/EtOAc (8:2 v/v): R$_f$ = 0.45; ^{1}H NMR (200 MHz, CDCl$_3$): δ = 7.57–7.40 (m, 5H), 4.27 (q, 1H, J = 7.2 Hz), 4.21 (q, 1H, J = 7.2 Hz), 3.57 (t, 2H), 2.57–2.27 (m, 2H), 2.05–1.80 (m, 2H), 1.26 (t, 3H, J = 7.2 Hz).

4.3.3 | 4-Chloro-2-(R/S)-phenylbutanenitrile (6)

Ethyl 4-chloro-2-(R/S)-cyano-2-phenylbutanoate (4.64 mmoL, 1 eq) was dissolved in CH$_3$OH (20 mL), and a saturated aqueous solution of K$_2$CO$_3$ (4 mL) was added at 0 °C. The reaction mixture was stirred at rt for 3 h, and HCl was added to pH 7. The mixture was partitioned with diethyl ether, the organic phase was washed with brine, dried over Na$_2$SO$_4$, and concentrated in vacuo to obtain a light-yellow oil. Yield: 75%; TLC C$_6$H$_{12}$/EtOAc (8:2 v/v): R$_f$ = 0.36; ^{1}H NMR (200 MHz, CDCl$_3$): δ = 7.38–7.27 (m, 5H), 4.14 (t, 1H), 3.72–3.48 (m, 1H), 2.45–2.22 (m, 1H), 1.73–1.40 (m, 2H).

4.3.4 | 5-Chloro-2-(R/S)-pentanenitrile (7)

Ethyl 5-chloro-2-(R/S)-cyano-2-phenylpentanoate (11.51 mmoL, 1 eq) was dissolved in CH$_3$OH (40 mL), and a saturated aqueous solution of K$_2$CO$_3$ (8 mL) was added at 0 °C. The reaction mixture was stirred at rt for 3 h, and HCl was added to pH 7. The mixture was transferred to a separatory funnel and partitioned with diethyl ether. The organic phase was washed with brine, dried over Na$_2$SO$_4$, and concentrated in vacuo to obtain a light-yellow oil. Yield: 61%; TLC C$_6$H$_{12}$/EtOAc (8:2 v/v): R$_f$ = 0.40; ^{1}H NMR (200 MHz, CDCl$_3$): δ = 7.40–7.33 (m, 5H), 3.82 (t, 1H), 3.57 (t, 2H), 2.15–1.94 (m, 4H).

4.3.5 | Ethyl 4-chloro-2-(R/S)-phenylbutanoate (8)

4-Chloro-2(R/S)-phenylbutanonitrile (3.46 mmoL, 1 eq) was added to a 1: 1 mixture of HCl (12 N) and CH$_3$CH$_2$OH, and the resulting suspension was stirred and refluxed for 24 h. After, the reaction mixture was concentrated under *vacuum*, transferred to a separatory funnel, and partitioned with CH$_2$Cl$_2$. The organic phase was washed with brine, dried on Na$_2$SO$_4$, and concentrated to obtain a colorless oil. Yield: 63%; TLC C$_6$H$_{12}$/

EtOAc (8:2 v/v): R$_f$ = 0.48; ^{1}H NMR (200 MHz, CDCl$_3$): δ = 7.39–7.27 (m, 5H), 4.15 (q, 1H, J = 7.4 Hz), 4.09 (q, 1H, J = 7.4 Hz), 3.87 (t, 1H), 3.57–3.43 (m, 1H), 2.59–2.42 (m, 1H), 2.35–2.17 (m, 1H), 1.77–1.74 (m, 1H), 1.20 (t, 3H, J = 7.4 Hz).

4.3.6 | Ethyl 5-chloro-2-(R/S)-phenylpentanoate (9)

5-Chloro-2-(R/S)-pentanenitrile (7.94 mmoL, 1 eq) was added to a 1:1 mixture of HCl (12 N) and CH$_3$CH$_2$OH, and the resulting suspension was stirred and refluxed for 24 h. Afterward, the reaction mixture was concentrated under vacuum, transferred to a separatory funnel, and partitioned with CH$_2$Cl$_2$. The organic phase was washed with brine, dried on Na$_2$SO$_4$, and concentrated to obtain a transparent oil. Yield: 52%; TLC C$_6$H$_{12}$/EtOAc (8:2 v/v): R$_f$ = 0.54; ^{1}H NMR (200 MHz, CDCl$_3$): δ = 7.38–7.27 (m, 5H), 4.18 (q, 1H, J = 7.4 Hz), 4.05 (q, 1H, J = 7.4 Hz), 3.58–3.51 (m, 3H), 2.30–2.19 (m, 1H), 2.00–1.93 (m, 1H), 1.79–1.68 (m, 2H), 1.22 (t, 3H, J = 7.4 Hz).

4.3.7 | Ethyl 4-((2R,6R,11R)-8-hydroxy-6,11-dimethyl-1,4,5,6-tetrahydro-2,6-methanobenzo[d]azocin-3(2H)-yl)-2-(R/S)-phenylbutanoate (10)

(−)-cis-N-normetazocine (2.17 mmoL, 1 eq) was dissolved in DMF (6 mL), and ethyl 4-chloro-2-(R/S)-phenylbutanoate (2.17 mmoL, 1 eq), NaHCO$_3$ (3.25 mmoL, 1.5 eq) and KI (catalytic quantity) were added. The reaction mixture was stirred at 65 °C for 72 h. After, the mixture was transferred to a separatory funnel and partitioned (EtOAc/H$_2$O). The organic phase was washed with brine, dried on Na$_2$SO$_4$, and concentrated under vacuum. The reaction crude was purified by flash chromatography (CH$_2$Cl$_2$/MeOH 95:5) to obtain an orange solid. Yield: 30%; Mp: 157–160 °C; $[\alpha]_D^{25}$ = −56.6° (c 1.1, EtOH); TLC CH$_2$Cl$_2$/MeOH (95:5 v/v) R$_f$ = 0.35; ^{1}H NMR (200 MHz, CDCl$_3$): δ = 7.30–7.19 (m, 5H), 6.82 (d, 1H J = 8.0 Hz), 6.63 (d, 1H J = 2.2 Hz), 6.53 (dd, 1H, J = 2.2, 8.0 Hz), 4.03 (q, 2H, J = 7.2 Hz), 3.56 (t, 1H, J = 7.1 Hz), 2.83–2.22 (m, 7H), 2.11–1.72 (m, 4H), 1.61–1.46 (m, 1H), 1.23 (s, 3H) 1.12 (t, 3H, J = 7.2 Hz), 0.75 (d, 3H, J = 7.0 Hz). (Figure S6) ^{13}C NMR (50 MHz, CDCl$_3$): δ = 173.87, 154.56, 142.79, 138.85, 129.01, 128.59, 128.14, 128.02, 127.85, 127.20, 113.24, 112.40, 60.84, 57.57, 52.54, 49.78, 45.87, 41.85, 41.49, 41.38, 40.85, 36.19, 33.42, 25.23, 23.30, 14.05. Anal (C$_{26}$H$_{33}$NO$_3$) C, H, N (Table S1).

4.3.8 | Ethyl 5-((2R,6R,11R)-8-hydroxy-6,11-dimethyl-1,4,5,6-tetrahydro-2,6-methanobenzo[*d*]azocin-3(2*H*)-yl)-2-(*R/S*)-phenylpentanoate (**11**)

(−)-*cis*-*N*-normetazocine (4.15 mmoL, 1 eq) was dissolved in DMF (6 mL) and ethyl 5-chloro-2-(*R/S*)-phenylpentanoate (4.15 mmoL, 1 eq), NaHCO$_3$ (6.23 mmoL, 1.5 eq) and KI (catalytic quantity) were added. The reaction mixture was stirred at 65 °C for 72 h. After, the mixture was transferred to a separatory funnel and partitioned (EtOAc/H$_2$O). The organic phase was washed with brine, dried on Na$_2$SO$_4$, and concentrated in vacuum. The reaction crude was purified by flash chromatography (CH$_2$Cl$_2$/MeOH 95:5) to obtain an orange solid. Yield: 46%; Mp: 161–164 °C; $[\alpha]_D^{25} = -54.2°$ (*c* 1.05, EtOH); TLC CH$_2$Cl$_2$/MeOH (95:5 *v/v*) R_f = 0.48; ^{1}H NMR (500 MHz, CDCl$_3$): δ = 7.56–7.54 (m, 2H), 7.41–7.36 (m, 3H), 6.91 (d, 1H, *J* = 10.0 Hz), 6.69 (d, 1H, *J* = 5.0 Hz), 6.59 (dd, 1H, *J* = 5.0, 10.0 Hz), 4.13–4.12 (m, 1H), 2.64–2.40 (m, 5H), 2.02–1.98 (m, 2H), 1.85–1.70 (m, 4H), 1.64–1.56 (m, 4H), 1.32 (s, 3H), 1.27–1.24 (m, 3H), 0.81 (d, 3H). (Figure S7) ^{13}C NMR (125 MHz, CDCl$_3$): δ = 167.60, 167.47, 155.91, 133.70, 133.30, 129.49, 129.44, 129.35, 129.33, 128.53, 126.00, 118.02, 114.43, 112.67, 85.11, 83.62, 63.56, 54.29, 54.25, 53.61, 53.47, 35.48, 35.09, 34.79, 29.73, 24.27, 13.74. Anal (C$_{27}$H$_{35}$NO$_3$) C, H, N (Table S1).

4.3.9 | 4-((2R,6R,11R)-8-hydroxy-6,11-dimethyl-1,4,5,6-tetrahydro-2,6-methanobenzo[*d*]azocin-3(2*H*)-yl)-2-(*R/S*)-phenylbutanoic acid (**12**)

1 N NaOH solution (3.06 mmoL, 11.3 eq) was added to ethyl 4-((2*R*,6*R*,11*R*)-8-hydroxy-6,11-dimethyl-1,4,5,6-tetrahydro-2,6-methanobenzo[*d*]azocin-3(2*H*)-yl)-2-(*R/S*)-phenylbutanoate (0.27 mmoL, 1 eq). The resulting suspension was vigorously stirred and refluxed at 110 °C for 5 h. After, the mixture was cooled at rt, transferred to a separatory funnel, and partitioned (CHCl$_3$/H$_2$O). A 1 N solution of HCl was added to the aqueous phase until a pH range of 5–6. The obtained yellow precipitate was separated from the aqueous phase by vacuum filtration. Yield: 43%, Mp: 192 °C dec; $[\alpha]_D^{25} = -42.6°$ (*c* 1.02, EtOH); TLC CH$_2$Cl$_2$/MeOH (95:5 *v/v*) R_f = 0.29; ^{1}H NMR (500 MHz, DMSO-*d$_6$*): δ = 8.49 (brs, 1H), 7.28–7.26 (m, 2H), 7.19–7.16 (m, 2H), 7.09–7.07 (m, 1H), 6.99 (d, 1H, *J* = 10.0 Hz), 6.81–6.79 (d, 1H, *J* = 10 Hz), 6.49–6.47 (dd, 1H, *J* = 10 Hz), 3.19–3.06 (m, 2H), 2.74–2.68 (m, 2H), 2.44–2.28 (m, 4H), 1.86–1.83 (m, 2H), 1.70–1.58 (m, 3H), 1.17–1.14 (m, 2H), 0.84–0.83 (m, 1H), 0.68 (d, 3H, *J* = 7.2 Hz). (Figure S8) ^{13}C NMR (125 MHz, DMSO-*d$_6$*): δ = 177.13, 172.88, 156.00, 144.82, 142.37, 128.08, 127.84, 127.70, 126.79, 125.62, 113.32,

112.12, 86.24, 67.55, 56.63, 52.94, 45.00, 41.97, 36.41, 33.00, 29.08, 25.47, 22.62, 13.64. Anal (C$_{24}$H$_{29}$NO$_3$) C, H, N (Table S1).

4.3.10 | 5–((2R,6R,11R)-8-hydroxy-6,11-dimethyl-1,4,5,6-tetrahydro-2,6-methanobenzo[*d*]azocin-3(2*H*)-yl)-2-(*R/S*)-phenylpentanoic acid (**13**)

1 N NaOH solution (10.53 mmoL, 11.3 eq) was added to ethyl 5-((2*R*, 6*R*, 11*R*)-8-hydroxy-6,11-dimethyl-1,4,5,6-tetrahydro-2,6-methanobenzo[*d*]azocin-3(2*H*)-yl)-2-(*R/S*)-phenylpentanoate (0.93 mmoL, 1 eq). The resulting suspension was vigorously stirred and refluxed at 110 °C for 5 h. After, the mixture was cooled at rt, transferred to a separatory funnel, and partitioned (CHCl$_3$/H$_2$O). A 1 N solution of HCl was added to the aqueous phase until a pH range of 5–6. The obtained yellow precipitate was separated from the aqueous phase by vacuum filtration. Yield: 52%; Mp: 195 °C dec; $[\alpha]_D^{25} = -40.9°$ (*c* 1.08, EtOH); TLC CH$_2$Cl$_2$/MeOH (95:5 *v/v*) R_f = 0.20; ^{1}H NMR (200 MHz, CD$_3$OD): δ = 7.47–7.22 (m, 5H), 7.05 (d, 1H, *J* = 10.0 Hz), 6.80 (d, 1H, *J* = 5.0 Hz), 6.72 (dd, 1H, *J* = 5.0, 10.0 Hz), 4.28–4.24 (m, 1H), 3.72–3.54 (m, 1H), 3.23–3.11 (m, 5H), 2.20–2.00 (m, 4H), 1.82–1.59 (m, 4H), 1.46 (s, 3H), 0.98 (d, 3H). (Figure S9) ^{13}C NMR (125 MHz, DMSO-*d$_6$*): δ = 177.57, 174.23, 161.29, 155.83, 142.97, 139.52, 128.41, 128.12, 127.77, 127.61, 127.30, 126.87, 113.48, 112.23, 94.66, 91.20, 72.87, 57.00, 50.97, 44.83, 30.95, 28.82, 24.98, 19.45, 13.47. Anal (C$_{25}$H$_{31}$NO$_3$) C, H, N (Table S1).

4.4 | Radioligand binding assays

The radioligand binding assays and the data analysis were performed as previously reported (Rita Turnaturi et al., 2022).

4.5 | Molecular modeling

4.5.1 | Structures preparation and minimization

All the molecules used in this study were built using Marvin Sketch (18.24, ChemAxon Ltd.). The PM6-D3H4 Hamiltonian, implemented in the MOPAC package (MOPAC2016 v. 18.151, Stewart Computational Chemistry, Colorado Springs), was then used to further optimize the 3D structures before the alignment for the docking calculations.

4.5.2 | Docking and molecular dynamics studies

Flexible ligands docking experiments were performed employing AutoDock implemented in YASARA, using the crystal structure of MOR (PDB code: 5C1M) (Huang et al., 2015), the crystal structure of DOR (PDB code: 4EJ4) (Granier et al., 2012) and crystal structure of KOR (PDB ID: 4DJH) (Wu et al., 2012) retrieved from the PDB_REDO Data Bank. A periodic simulation cell with boundaries extending 5 Å (Duan et al., 2003) from the surface of the ligand was employed.

The molecular dynamics (MD) simulations of the complexes were performed with the YASARA structure package according to our previously reported procedures (Floresta et al., 2019; Patamia et al., 2023).

CONFLICT OF INTEREST STATEMENT
The authors declare no competing financial interest.

DATA AVAILABILITY STATEMENT
The data that support the findings of this study are available on request from the corresponding author. The data are not publicly available due to privacy or ethical restrictions.

ORCID
Antonio Rescifina [ORCID] https://orcid.org/0000-0001-5039-2151

REFERENCES
Brine, G. A., Berrang, B., Hayes, J. P., & Carroll, F. I. (1990). An improved resolution of (+/−)-cis-N-Normetazocine. *Journal of Heterocyclic Chemistry*, 27(7), 2139–2143. https://doi.org/10.1002/jhet.5570270753

Cheng, C. Y., Lu, H. Y., Lee, F. M., & Tam, S. W. (1990). Synthesis of (1′, 2′-trans)-3-Phenyl-1-[2′-(N-pyrrolidinyl)cyclohexyl]-Pyrrolid-2-ones as K-selective opiates. *Journal of Pharmaceutical Sciences*, 79(8), 758–762. https://doi.org/10.1002/jps.2600790821

Duan, Y., Wu, C., Chowdhury, S., Lee, M. C., Xiong, G. M., Zhang, W., Yang, R., Cieplak, P., Luo, R., Lee, T., Caldwell, J., Wang, J., & Kollman, P. (2003). A point-charge force field for molecular mechanics simulations of proteins based on condensed-phase quantum mechanical calculations. *Journal of Computational Chemistry*, 24(16), 1999–2012. https://doi.org/10.1002/jcc.10349

Floresta, G., Gentile, D., Perrini, G., Patamia, V., & Rescifina, A. (2019). Computational tools in the discovery of FABP4 ligands: A statistical and molecular modeling approach. *Marine Drugs*, 17(11), 624. https://doi.org/10.3390/md17110624

Gentile, D., Coco, A., Patamia, V., Zagni, C., Floresta, G., & Rescifina, A. (2022). Targeting the SARS-CoV-2 HR1 with small molecules as inhibitors of the fusion process. *International Journal of Molecular Sciences*, 23(17), 10067. https://doi.org/10.3390/ijms231710067

Granier, S., Manglik, A., Kruse, A. C., Kobilka, T. S., Thian, F. S., Weis, W. I., & Kobilka, B. K. (2012). Structure of the delta-opioid receptor bound to naltrindole. *Nature*, 485(7398), 400–404. https://doi.org/10.1038/nature11111

Huang, W. J., Manglik, A., Venkatakrishnan, A. J., Laeremans, T., Feinberg, E. N., Sanborn, A. L., Kato, H. E., Livingston, K. E., Thorsen, T. S., Kling, R. C., Granier, S., Gmeiner, P., Husbands, S. M., Traynor, J. R., Weis, W. I., Steyaert, J., Dror, R. O., & Kobilka, B. K. (2015). Structural insights into mu-opioid receptor activation. *Nature*, 524(7565), 315–321. https://doi.org/10.1038/nature14886

Parenti, C., Tumaturi, R., Arico, G., Gramowski-Voss, A., Schroeder, O. H. U., Marrazzo, A., Prezzavento, O., Ronsisvalle, S., Scoto, G. M., Ronsisvalle, G., & Pasquinucci, L. (2013). The multitarget opioid ligand LP1's effects in persistent pain and in primary cell neuronal cultures. *Neuropharmacology*, 71, 70–82. https://doi.org/10.1016/j.neuropharm.2013.03.008

Pasquinucci, L., Parenti, C., Georgoussi, Z., Reina, L., Tomarchio, E., & Turnaturi, R. (2021). LP1 and LP2: Dual-target MOPr/DOPr ligands as drug candidates for persistent pain relief. *Molecules*, 26(14), 4168. https://doi.org/10.3390/molecules26144168

Pasquinucci, L., Parenti, C., Turnaturi, R., Arico, G., Marrazzo, A., Prezzavento, O., & Ronsisvalle, G. (2012). The benzomorphan-based LP1 ligand is a suitable MOR/DOR agonist for chronic pain treatment. *Life Sciences*, 90(1–2), 66–70. https://doi.org/10.1016/j.lfs.2011.10.024

Pasquinucci, L., Prezzavento, O., Marrazzo, A., Amata, E., Ronsisvalle, S., Georgoussi, Z., Fourla, D. D., Scoto, G. M., Parenti, C., Aricò, G., & Ronsisvalle, G. (2010). Evaluation of N-substitution in 6,7-benzomorphan compounds. *Bioorganic & Medicinal Chemistry*, 18(14), 4975–4982. https://doi.org/10.1016/j.bmc.2010.06.005

Pasquinucci, L., Turnaturi, R., Montenegro, L., Caraci, F., Chiechio, S., & Parenti, C. (2019). Simultaneous targeting of MOR/DOR: A useful strategy for inflammatory pain modulation. *European Journal of Pharmacology*, 847, 97–102. https://doi.org/10.1016/j.ejphar.2019.01.031

Pasquinucci, L., Turnaturi, R., Prezzavento, O., Arena, E., Arico, G., Georgoussi, Z., Parenti, R., Cantarella, G., & Parenti, C. (2017). Development of novel LP1-based analogues with enhanced delta opioid receptor profile. *Bioorganic & Medicinal Chemistry*, 25(17), 4745–4752. https://doi.org/10.1016/j.bmc.2017.07.021

Patamia, V., Floresta, G., Zagni, C., Pistarà, V., Punzo, F., & Rescifina, A. (2023). 1, 2-Dibenzoylhydrazine as a multi-inhibitor compound: A morphological and docking study. *International Journal of Molecular Sciences*, 24(2), 1425. https://doi.org/10.3390/ijms24021425

Pathan, H., & Williams, J. (2012). Basic opioid pharmacology: An update. *British Journal of Pain*, 6(1), 11–16. https://doi.org/10.1177/2049463712438493

Rescifina, A., Zagni, C., Mineo, P. G., Giofrè, S. V., Chiacchio, U., Tommasone, S., Talotta, C., Gaeta, C., & Neri, P. (2014). DNA recognition with polycyclic-aromatic-hydrocarbon-presenting calixarene conjugates. *European Journal of Organic Chemistry*, *2014*(34), 7605–7613. https://doi.org/10.1002/ejoc.201403050

Ricarte, A., Dalton, J. A. R., & Giraldo, J. (2021). Structural assessment of agonist efficacy in the mu-opioid receptor: Morphine and fentanyl elicit different activation patterns. *Journal of Chemical Information and Modeling*, *61*(3), 1251–1274. https://doi.org/10.1021/acs.jcim.0c00890

Szczepańska, K., Podlewska, S., Dichiara, M., Gentile, D., Patamia, V., Rosier, N., Mönnich, D., Ruiz Cantero, M. C., Karcz, T., Łażewska, D., Siwek, A., Pockes, S., Cobos, E. J., Marrazzo, A., Stark, H., Rescifina, A., Bojarski, A. J., Amata, E., & Kieć-Kononowicz, K. (2021). Structural and molecular insight into piperazine and piperidine derivatives as histamine H3 and sigma-1 receptor antagonists with promising antinociceptive properties. *ACS Chemical Neuroscience*, *13*(1), 1–15. https://doi.org/10.1021/acschemneuro.1c00435

Turnaturi, R., Chiechio, S., Pasquinucci, L., Spoto, S., Costanzo, G., Dichiara, M., Piana, S., Grasso, M., Amata, E., & Marrazzo, A. (2022). Novel N-normetazocine derivatives with opioid agonist/Sigma-1 receptor antagonist profile as potential analgesics in inflammatory pain. *Molecules*, *27*(16), 5135. https://doi.org/10.3390/molecules27165135

Turnaturi, R., Marrazzo, A., Parenti, C., & Pasquinucci, L. (2018). Benzomorphan scaffold for opioid analgesics and pharmacological tools development: A comprehensive review. *European Journal of Medicinal Chemistry*, *148*, 410–422. https://doi.org/10.1016/j.ejmech.2018.02.046

Varrica, M. G., Zagni, C., Mineo, P. G., Floresta, G., Monciino, G., Pistarà, V., Abbadessa, A., Nicosia, A., Castilho, R. M., & Amata, E. (2018). DNA intercalators based on (1, 10-phenanthrolin-2-yl) isoxazolidin-5-yl core with better growth inhibition and selectivity than cisplatin upon head and neck squamous cells carcinoma. *European Journal of Medicinal Chemistry*, *143*, 583–590. https://doi.org/10.1016/j.ejmech.2017.11.067

Vicario, N., Pasquinucci, L., Spitale, F. M., Chiechio, S., Turnaturi, R., Caraci, F., Tibullo, D., Avola, R., Gulino, R., & Parenti, C. (2019). Simultaneous activation of mu and Delta opioid receptors reduces allodynia and astrocytic connexin 43 in an animal model of neuropathic pain. *Molecular Neurobiology*, *56*(11), 7338–7354. https://doi.org/10.1007/s12035-019-1607-1

Wu, H., Wacker, D., Mileni, M., Katritch, V., Han, G. W., Vardy, E., Liu, W., Thompson, A. A., Huang, X. P., & Carroll, F. I. (2012). Structure of the human *κ*-opioid receptor in complex with JDTic. *Nature*, *485*(7398), 327–332. https://doi.org/10.1038/nature10939

Zádor, F., Király, K., Essmat, N., & Al-Khrasani, M. (2022). Recent molecular insights into agonist-specific binding to the mu-opioid receptor. *Frontiers in Molecular Biosciences*, *9*, 900547. https://doi.org/10.3389/fmolb.2022.900547

SUPPORTING INFORMATION

Additional supporting information can be found online in the Supporting Information section at the end of this article.